^{4}He ordering transition on single-leaf pyrolytic graphite: A microcalorimetry study

J. H. Campbell* and Michael Bretz
Department of Physics, University of Michigan, Ann Arbor, Michigan 48109
(Received 11 February 1985)

We have developed an ac microcalorimeter for the thermodynamic study of adsorbed gases on a single cleaved leaf of pyrolytic graphite. Our sensitivity of about 0.1 nJ/deg was sufficient to probe details of the ^{4}He ordering transition. After *in situ* baking of the sample we found heat-capacity peaks comparable to those measured on the best exfoliated graphite substrates. The phase diagram near ordering is narrower than previously measured and a critical analysis yields asymmetric peaks: The low-T side diverges logarithmically for the six coverages analyzed between 0.0633/Å^2 and 0.0649/Å^2 while the high-T side of the peak displays a power-law divergence. The critical-heat-capacity exponent α in this coverage range drops from 0.48 (stronger than that in the three-state Potts model) to -0.07 (slightly cusped). We interpret the narrow ordered-phase region as reflecting our excellent film geometry and the unexpected nonuniversality as caused by residual impurity, rather than size-limiting effects. Additional ac calorimetry studies should complement adsorbed-film single-crystal diffraction research.

I. INTRODUCTION

The discovery of sharp monolayer phase transitions in the isotherms of Thomy and Duval[1] and in the heat-capacity data of Bretz and Dash[2] caused exfoliated graphite to become the standard substrate for physical-adsorption studies. Various types of exfoliates—Grafoil, Papyx, foam, uncompressed (worms), *ZYX* (Ref. 3), and single-crystal exfoliates (Ref. 4)—have since been used for optimizing the surface-to-volume ratio, crystalline orientation, thermal conductivity, gas-penetration times, and/or microcrystalline size as needed for the particular experimental technique. It became apparent early on that large surface areas were inversely correlated with the size of single-crystal regions in the exfoliates. Grafoil, for instance, possesses a surface area of ~ 20 m^2/g with ~ 150-Å microcrystallites[5] while *ZYX* has only 2.8 m^2/g but ≥ 600-Å crystallites.[6] Since two-dimensional (2D) crystallite size limits the resolution of monolayer phase transitions, a continuing problem for experimentalists has been to obtain sufficient area for a good signal-to-noise ratio while maintaining adequate resolution. A few techniques like low-energy electron diffraction (LEED) use single cleaved crystals[7] while others such as x-ray scattering have developed sufficiently that adsorption studies on single crystals are now possible.[8] We have adopted ac calorimetry[9] to investigate monolayer films and demonstrate that monolayer thermodynamics can also be studied on cleaved single-crystal graphite surfaces.[10]

In Fig. 1 we present a global phase diagram of monolayer ^{4}He adsorbed on graphite.[11,12] At low coverages (<0.06 atoms/Å^2) and temperatures (≤ 1.5 K) the 2D fluid coexists with a registered solid.[13] For a narrow region at intermediate coverages, 0.06–0.07 atoms/Å^2, a completely registered (or ordered) phase occurs below about 2.9 K. Here, helium atoms reside in the surface potential wells of the graphite basal plane. For higher coverages an incommensurate solid displaces the registered solid below about 2 K. On compression, this partially oriented solid stabilizes, causing the melting line to rise appreciably in temperature, finally reaching 9 K at monolayer completion. Figure 2 shows the specific-heat signatures for these melting and ordering transitions as measured on *ZYX* (Ref. 14) and foam (Ref. 13), respectively. The melting peak, which grows stronger toward monolayer completion, is consistent with a first-order transition that has been rounded by inhomogeneity effects,[13] while the large 3-K ordering peak has a second-order character.[12]

It has been suggested that the helium ordering transi-

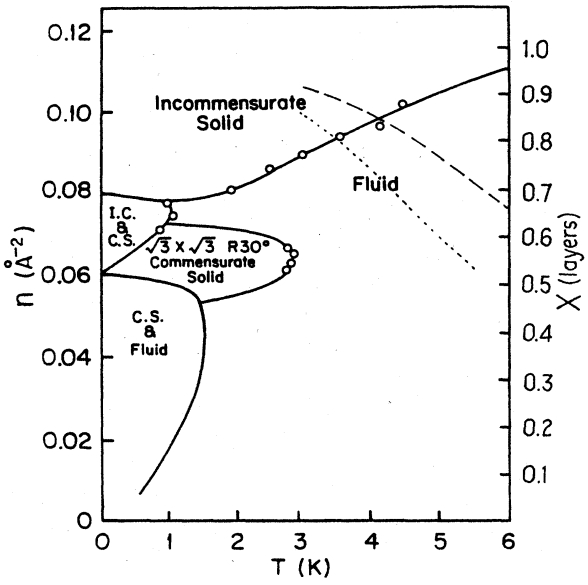

FIG. 1. Monolayer phase diagram of ^{4}He on graphite. Dotted line estimates 1% film depletion and dashed line bounds high-temperature region of ac calorimeter breakdown.

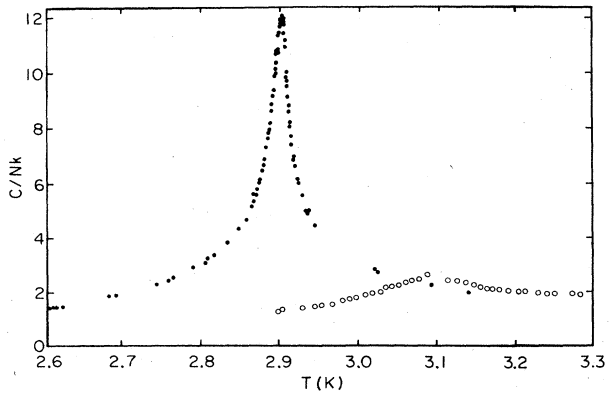

FIG. 2. ^{4}He ordering peak at critical coverage on *ZYX* graphite (Ref. 14) (●) and melting peak of incommensurate solid (Ref. 13) (○, enlarged 2×).

tion corresponds to the three-state Potts model in 2D, a model of fundamental theoretical interest.[15] Critical analysis of this specific-heat peak gives an exponent α of 0.36 ± 0.02 on *ZYX* (Ref. 14) and 0.28 ± 0.02 on foam (Ref. 16). These values straddle the theoretical Potts value of $\alpha=\frac{1}{3}$.[17] More recently, Huse and Fisher[18] proposed that the presence of both heavy- and light-density domain walls could cause an alteration of ordering transitions on graphite to include chiral behavior. They predict domain-wall wetting, a change in melting exponents from Potts values, and a multicritical point.

We took heat-capacity data for coverages near ordering in the temperature range 2—7 K and also made some runs close to monolayer completion to locate the melting transition and to observe desorption at higher T. Our principal interest was to determine the sensitivity of the ordering transition's critical properties to the geometry of the adsorption environment. Instead of using exfoliates, as in past experiments, we worked with a cleaved single crystal of highly oriented pyrolitic graphite (HOPG) (Ref. 19) to avoid the presence of adsorption chambers and damaged microcrystals. This substrate presents a slab geometry and has crystal facets of up to 1 μm in extent.

II. EXPERIMENTAL ASPECTS

A. The ac heat-capacity technique

We used the steady-state ac calorimetry technique developed by Sullivan and Seidel for measuring small samples.[9] A sample with internal heat capacity C_s and thermal conductance K_s communicates with the temperature bath T_b through a weak thermal link having conductance K_b. We chose heater and thermometer which maximized contact conductances K_H,K_θ and minimized the heat capacities C_H and C_θ. Applying an ac voltage of frequency $\omega/2$ to the heater raises the sample above T_b, where it oscillates about a steady-state offset temperature. The rms magnitude of these oscillations, T_{ac}, depends on ω, the thermal time constants, and the sample heat capacity C_s, through the relation

$$T_{ac}=\frac{P}{\sqrt{2}\omega C_s}[1+(\omega\tau_1)^{-2}+(\omega\tau_2)^2]^{-1/2}\ . \tag{1}$$

Here, P is the peak power to the ac heater (at frequency ω) and $\tau_1=C_s/K_b$ and τ_2 are the weak link and effective internal cell time constants, respectively. T_{ac} shifts out of phase, with respect to the heater oscillations, by an amount

$$\gamma\simeq\arctan\{[(\omega\tau_1)^{-1}-\omega\tau_2]^{-1}\}\ . \tag{2}$$

One always measures the frequency profile to determine an operating frequency within a "plateau" region where neither τ_1 nor τ_2 dominates T_{ac}. For frequencies on the plateau, Eq. (2) simplifies to

$$T_{ac}\cong\frac{P}{\sqrt{2}\omega C_s}\ , \tag{3}$$

so the heat capacity C_s can be easily calculated. In practice, the weak link, heater, thermometer, and addenda must be chosen carefully to match the thermal diffusion lengths, $l=\sqrt{2\kappa/\omega\rho c}$, of each material of the ac cell (where ρ is density, κ is thermal conductivity, and c is the specific heat). The appropriate operating frequency can be determined by scanning ωT_{ac} and can be maintained by monitoring γ to ensure that one has not shifted off the plateau.

B. The ac calorimeter

The calorimeter was constructed from cleaved monochrometer-grade HOPG. Blanks of 5.33 ± 0.03 mm on edge and 6.3 ± 1.3 μm thickness were cut from tear- and crease-free regions of the lamina. Three evaporator masks for depositing insulating layer, heater, and leads were prepared from 25-μm aluminum foil by a photolithographic process. Masks were positioned within 0.2 mm of the HOPG surface and blanks heated for 1 h at over 100 °C in 10^{-5} Torr before evaporations. Ion-bombardment cleaning preceded the first evaporation. Aluminum was deposited on the hot HOPG at $\simeq$60 Å/sec to a thickness of 1 μm, as measured by a quartz-crystal monitor. Without breaking vacuum, the substrate was raised to 200 °C and SiO evaporated over the aluminum at 15 Å/sec to 0.5 μm, using a baffled effusion source.[20] These films were then annealed at 275 °C for 1 h. After changing masks, reevacuating, and reheating the graphite, a base layer of 200 Å of NiCr and then 0.5 μm of gold were evaporated to form thermometer leads and heater. Then, another 200 Å of gold was evaporated through a serpentine mask to give a heater of about 1000 Ω resistance. An Electrodag[21] strip of roughly 0.1 mm×0.2 mm×0.006 mm was painted onto the calorimeter to serve as a thermometer. The leaf was baked in vacuum at 275 °C to drive off paint binder and a top film of SiO was evaporated to a thickness of 3000 Å for passivation before a final annealing. Three 18-μm gold-wire leads were thermocompression-bonded to small uncoated gold tabs. Diagrams of the ac calorimeter are shown in Fig. 3. A cylindrical copper chamber filled and lined with 65 Grafoil disks, which were previously baked in high vacuum to 1000 °C, enclosed the calorimeter. Holes were

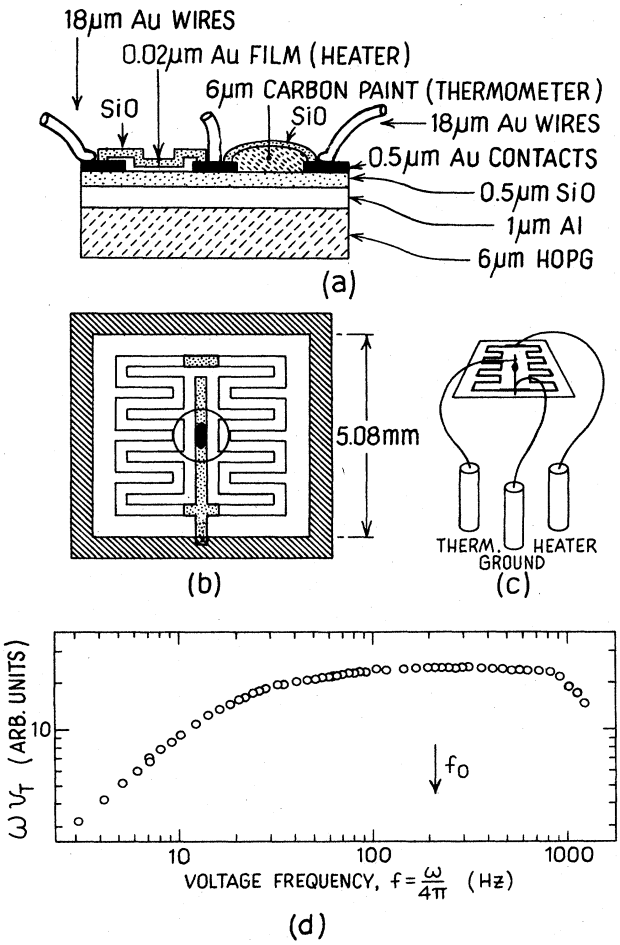

FIG. 3. Calorimeter design: (a) cross sectional view, (b) heater evaporation pattern and carbon-dot thermometer (region of SiO passivation is circled), (c) mounting to holder, and (d) frequency response of mounted cell showing operating frequency of heater voltage. v_T is the ac voltage response of the biased-temperature thermometer.

punched in each of the 0.8-mm-thick disks and they were staggered to form an "optically dense" pumping path from fill line to calorimeter. The three gold leads were attached to a standard feedthrough, which also acted as a mount for the calorimeter. To avoid solder-flux contamination, final assembly was made with stainless-steel compression seals.

C. Procedures

The ballast-cell temperatures were monitored by a directly mounted carbon resistor which served as the primary thermometer for the experiment. This was carefully calibrated over the range 2.4 to 4.2 K against the vapor pressure of the ^{4}He bath using the T58 temperature scale.[22] A recently calibrated capacitance manometer was used for pressure measurements. Monolayer capacity, which defines $x=1$ for the Grafoil-cell disks, was found to be 16 cm^3 (STP) by the point-"B" determination[12] of a 4.3-K ^{4}He isotherm.

A Z80-based microcomputer[23] recorded electrical signals through a 16-channel, 12-bit analog-to-digital converter board. The dc or "background" temperature of the ballast cell was measured with an in-house-built ac bridge and phase-sensitive detector. Temperatures could be determined to ± 15 μK at 3 K or controlled within 100 μK with a proportional feedback circuit.

The ac temperature of the calorimeter was measured with the carbon-paint thermometer. The thermometer was biased with a constant current supplied by a 4-V mercury battery and two 1-MΩ metal-film resistors, which were heat-sunk to the liquid-helium vacuum-can flange. Voltage fluctuations were sensed with a high-quality vector lock-in amplifier,[24] referenced in the $2f$ mode to the heater oscillator. Both in-phase and quadrature signal components were digitized and recorded. The heater resistance was stable at 800 Ω below about 8 K.

A frequency scan of ac-thermometer voltage times frequency versus heater oscillator frequency was taken at 3K as shown in Fig. 3(d). The ac calorimeter possessed a plateau over at least one decade in frequency. Low-frequency rolloff below 30 Hz corresponds to a weak link thermal time constant of $\tau_1 = 3$ msec. The high-frequency falloff is not due to internal cell conductivity problems, but to a limitation of our low-frequency lock-in detector card.

The assembled cell was pumped and baked for 1 d at 240 °C prior to cooldown. The high-temperature resistances of heater and thermometer were also noted.

III. PRESENTATION AND ANALYSIS OF DATA SET I

Initially we took data for several widely spaced submonolayer coverages from $x=0.55$ to 0.90 in the range 2—7 K as presented in Fig. 4. On this scale, $\lesssim 1$ μJ/K, all the data at lower temperatures fall along the bare calorimeter heat capacity, with large coverage-dependent shoulders appearing at higher T. Clearly, desorption of helium atoms from the calorimeter leaf causes these shoulders. Subsequent rises above the shoulders signal a thermal shorting of the weak link by the desorbed gas. Upon increasing the heater power by a factor of 4 from 0.5 to 2.0 μW, the dc offset temperature of the leaf was raised far enough above the Grafoil ballast temperature

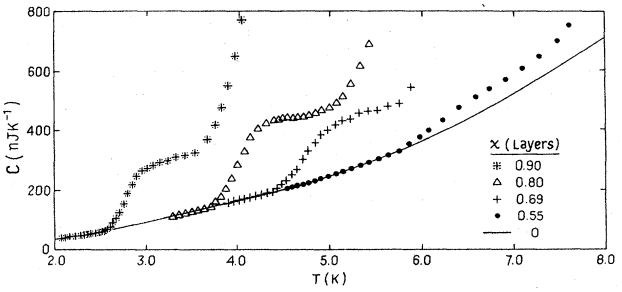

FIG. 4. Total heat-capacity signal for set-I data. Solid line is heat capacity of bare calorimeter.

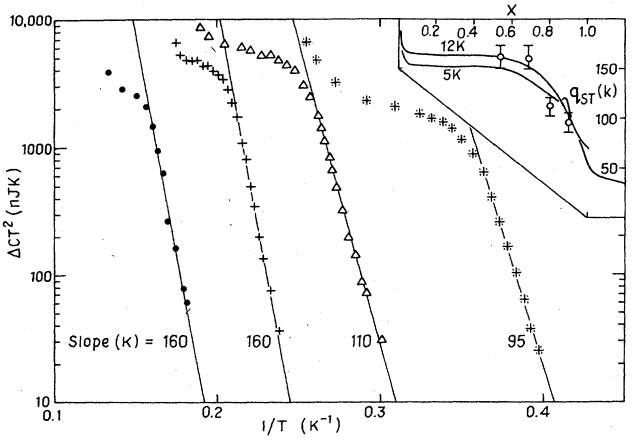

FIG. 5. Activation energy plot. ΔC is the film heat capacity after subtracting off the bare-calorimeter signal. Lines through data sets (same symbols as Fig. 4) are best fits. Slopes of these fits are equal to the heats of adsorption. Inset: isosteric heat of adsorption for ^{4}He monolayers on Grafoil (Ref. 25). Symbols represent slopes from main figure.

(25 to 100 mK) that differential gas pumping became apparent. Therefore, we have technical limits on the size of the dc offset at high temperatures and coverages. (No differential pumping problems are anticipated for data near the ordering transition since the vapor pressure is vanishingly small.)

An approximate heat of adsorption, q, can be extracted by subtracting off the bare calorimeter signal and replotting the Fig. 4 data as $\log(T^2C)$ versus $1/T$ in Fig. 5. The slope of the straight line, fitted through the data points at low film depletion, gives q. The inset of Fig. 5 compares these q's to the isosteric heats of adsorption, q_{st}, on Grafoil at 5 and 12 K found by Elgin and Goodstein.[25] Our q's approximate their curves, indicating that the helium-film platings on the microcalorimeter leaf at low dc-offset temperatures are close to q_{st} for the associated Grafoil ballast. The dotted line in Fig. 1 represents the approximate regions where 1% film depletion occurs (assuming 50% depletion at the knees of Fig. 4) and the dashed line indicates the upper temperature and coverage limits of our ac technique.[26]

From geometry, we expect the specific heat of an ideal 2D gas to be about 2.4 nJ/K at the ordering coverage (0.0635 atoms/Å^2). From the areas under the desorption curves in Fig. 4, we estimate the 2D gas specific heat to be about 1.2 nJ/K. These values are in moderate agreement. Atoms desorbing from the SiO-covered side of the leaf should add a contribution of similar size to the desorption heat-capacity signal. The heat of adsorption for ^{4}He on SiO is evidently so large that desorption occurs at temperatures higher than our calorimeter limit.

IV. DATA SET II

Although we expected to observe ordering and monolayer solid melting peaks in the lower-temperature data of Fig. 4, only monotonic heat capacities were obtained. Therefore, we recleaned the HOPG leaf through a series of *in situ* bakeouts. By applying up to 4.5 V across the vapor-deposited heater, we raised the temperature of the leaf to about 100 °C (as measured by the heater resistance) while keeping the surrounding Grafoil ballast and cell holder below 6K. After approximately 10 h of such heating we readmitted helium gas, letting it anneal for 1 d at 10 K. As the cell cooled to 3 K over 2—3 h, we obtained data for the three coverages as shown in Fig. 6. A well-formed ordering peak was now observed! Its presence demonstrates the importance of *in situ* bakeout procedures in single-leaf experiments. The heat capacity of the bare leaf, typically measured at about 70 points over the temperature interval from 2.4 to 3.4 K, was fitted with an eighth-order polynomial. Fit residuals indicate a resolution of ± 0.1 nJ/K. We found good reproducibility of the heat-capacity points when varying heater power by an order of magnitude, taking data nonsequentially in temperature and after warming the cryostat temporarily to liquid-nitrogen temperatures. We have also confirmed that at 3 K we were operating in the frequency plateau region of the microcalorimeter.

Data between 1.5 and 8 K for other coverages closer to monolayer completion ($x=0.62$, 0.74, and 0.86) were taken with the hope of observing 2D melting, but only monotonic heat capacities were found. From a comparison of Figs. 2 and 6, we evidently have marginal sensitivity to discriminate the melting signature at 0.74 and 0.86 layers.

On the other hand, our ordering peak at $x=0.554$ is sharp enough that a critical analysis of the data was performed. We used the method of Lederman, Salamon, and Shacklette[27] for sequential parameter determination for a specific-heat divergence of the form

$$C^{\pm}=A^{\pm}|t|^{-\alpha}+B^{\pm}+ct\ . \tag{4}$$

Here + or − refers to the high or low side of T_c and $t=(T/T_c-1)$. Universality[28] requires the specific-heat exponent α to be the same both above and below T_c. This analysis method, as applied to the helium ordering peak on foam and *ZYX* graphite, has already been described.[14,16] It will not be further discussed here, except to say that for better analysis statistics the data below T_c were shifted and folded into the data above T_c to give a

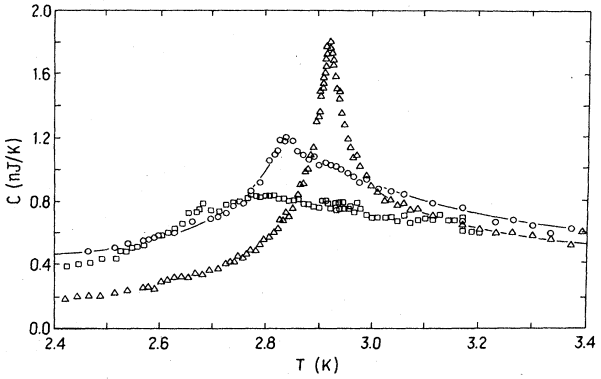

FIG. 6. Set-II data. Heat capacity after background subtraction for films with $x=0.523$ (□), 0.547 (○), and 0.554 (△).

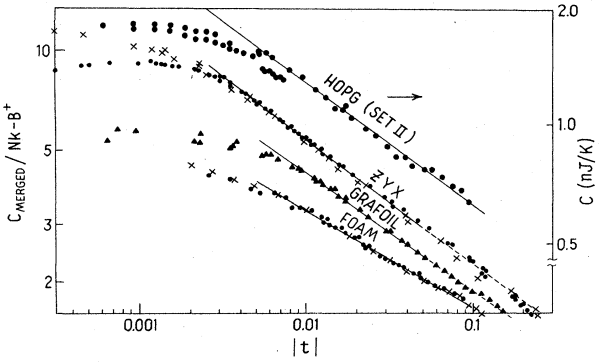

FIG. 7. Merged specific heat of ^{4}He vs reduced temperature for critical region of coverage $x=0.554$. Lines are best fits through the merged data. For clarity, the Grafoil and foam data have been offset vertically.

merged heat capacity called C_M.

Figure 7 presents our merged data at 0.554 layer as a $\log(C_M/Nk_B\text{-}B^+)$-versus-$\log(t)$ plot. From the slope of the straight-line fit, spanning over 1 decade in reduced temperature, we find that $T_c=2.917\pm0.005$ K and $\alpha\cong0.32\pm0.05$. Also included in Fig. 7 are similar analyses for ^{4}He on foam,[16] where α was determined to be 0.28 ± 0.02, *ZYX* (Ref. 14) with $\alpha=0.36\pm0.02$, and Grafoil where α was originally thought to be zero.[12,29] A comparison of reduced temperatures at peak rounding shows that our $x=0.544$ ordering peak on HOPG is similar to peaks on Grafoil. The ratio of peak height to heat capacity at 3.3 K (which is far from T_c) is 3.3 for Grafoil and 3.1 for our peak. This agreement with the Grafoil results was previously communicated.[10] However, the value of $Nk_B\cong0.60$ nJ/K, determined from the heat-capacity comparison, is only $\frac{1}{2}$ of that estimated from desorption (Sec. III). It is apparent that a large fraction of the adsorbed atoms are immobile and therefore are not participating in the ordering transition.

V. DATA SET III

At this point we attempted an alternate cleaning method. With the cryostat at room temperature the leaf was heated to about 170°C for 2 d in vacuum. The cell was closed off and the cryostat again cooled *while maintaining the HOPG leaf at an elevated temperature.* With the cryostat at 10 K, *in situ* baking continued for another day before we calibrated resistors and retook bare calorimeter data. Again, we inserted a coverage of $x=0.554$, but the peak now appeared at 2.86 K. Apparently the protecting Grafoil ballast collected some impurities during the previous 2 months, thereby causing a noticeable coverage shift.

We made six consecutive runs 1–6 at closely spaced decreasing coverages in the vicinity of the ordering peak. All runs were made under identical experimental and instrumental conditions so later careful comparisons could

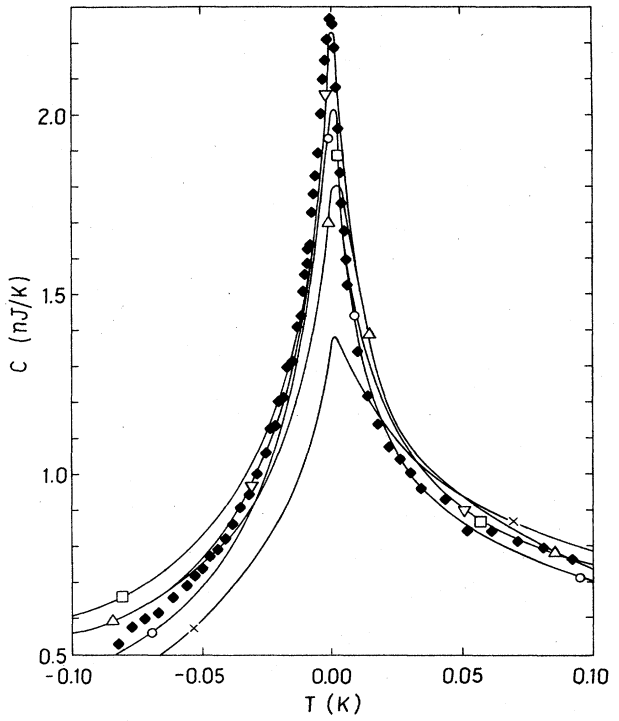

FIG. 8. Set-III data. Heat capacity of adsorbed film vs reduced temperature $(T-T_c)$ for data from runs 1 (×), 2 (△), 3 (□), 4 (◆), 5 (▼), and 6 (○). For clarity, data points are only given for run 4. Peak shapes for other data runs are indicated by lines through the respective data.

be made. The heat capacity of data runs 1–6 are plotted versus the reduced temperature in Fig. 8. The T_c's were determined from least-squares fits (see next section). For clarity, only data from run 4 are given in the figure; the lines indicate data from other runs. The peak wings overlap (except for data from run 1) and the peak heights (and T_c's) grow to a maximum for data of run 4. Note that we plot the *total* heat capacity in nJ/K, *not* the specific heat in Boltzmanns.

In order to properly assess the relative coverage shift between data sets II and III, we plotted a composite phase diagram of the ordering region for ^{4}He, as measured on three exfoliated graphites—Grafoil (×),[12] foam (*),[16] and *ZYX* (+).[15,30] A dashed line follows these composite data (top curve of Fig. 9). Sets II and III (○ in the figure) were shifted in coverage until T_c for the highest peaks of each set lay on the composite phase boundary. This placement required a $-0.0006/\text{Å}^2$ shift for set II and a $+0.0013/\text{Å}^2$ shift for set III from the nominal value of n_c, determined by the monolayer capacity.

A major discrepancy exists between the width of the ordering region for ^{4}He on the exfoliates and on HOPG. If our coverage placement is correct, the phase diagram for ^{4}He on HOPG is 2–3 times narrower than on exfoliated graphite! This placement is confirmed by a uniform and symmetric growth of peak heights as coverage approaches n_c from either side (◇ in Fig. 9).

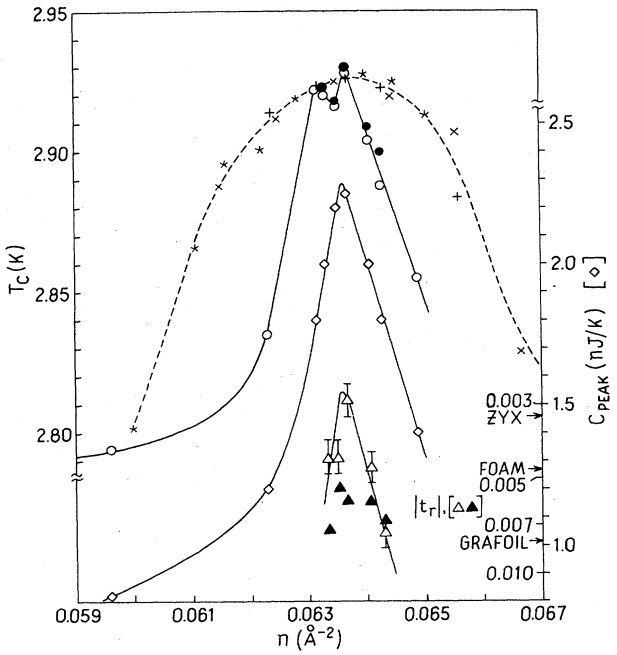

FIG. 9. Coverage plot. Top curve, phase diagram of the ^{4}He ordering transition region. Symbols are ×, Grafoil (cell *B* of Ref. 12); *, foam (Ref. 16); +, *ZYX* (Ref. 14) (offset by 20 mK) (Ref. 30). Dotted phase line guides the eye. Curve (○,●), T_c vs coverage for this study. Curve ◇, heat-capacity-peak height vs coverage. Use scale at right. Curve △,▲, reduced temperatures at onset of peak rounding. Inverted log scale at right also shows onsets of rounding for ^{4}He on exfoliated graphites. Error bars correspond to data spacing at rounding. Solid symbols are for $t<0$.

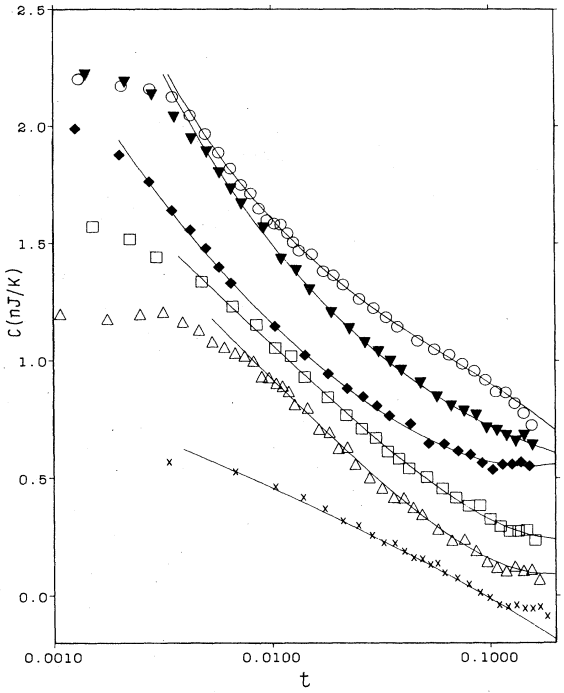

FIG. 10. Set-III high-T fits. Heat capacity (nJ/K) for $t>0$ vs log of reduced temperature. Lines are multiparameter power-law fits to data. For clarity, data have been offset vertically. 1 (×, down by 0.8 nJ/K), 2 (△, −0.6), 3 (□, −0.4), 4 (◆, −0.2), 5 (▼, unshifted), and 6 (○, up by 0.2).

VI. SET-III CRITICAL ANALYSIS

The analysis technique of Lederman *et al.* was attempted on data set III, but a satisfactory merging of heat-capacity data above and below T_c was not possible. This difficulty can be clarified by referring to Fig. 8, where close inspection shows that the highest peaks are *not* symmetrical about T_c. We thus proceeded to separately analyze the high- and low-temperature sides of the ordering peak, using a modification of Eq. (4) with the five parameters $A^{\pm}$, $B^{\pm}$, $C^{\pm}$, T_c (T_c'), and α (α') for fits above (below) T_c,

$$C^{\pm}=\frac{A^{\pm}(|t|^{-\alpha}-1)}{\alpha}+B^{\pm}+c^{\pm}t\ . \tag{5}$$

Data manipulation and analysis were accomplished using RS/1, The Research System,[31] a software package available on our Vax 11/780 computer. RS/1's least-squares-fitting routine uses the Marquardt-Levenberg method with 64-bit precision and provides regression results, parameter significance, and analysis of variance. We used a convergence criteria of <0.0001 improvement for the sum of squares (SS) between subsequent iterations, measuring the goodness of fit with a multiple r^2 coefficient (regression SS divided by total SS; typical values were $r^2\simeq 0.999$). Data weights other than unity were tried and found not to affect the analysis results appreciably.

The data and resulting fits for $t>0$ are given in the semilog plot of Fig. 10. For clarity, the data for different coverages have been offset vertically by amounts specified in the figure caption. Fits for data from runs 1—3 are approximately linear in the range $t<.05$, while a distinct upward curvature appears in the fits for data from runs 4—6. This curvature measures α and, as coverage decreases, α rises rapidly from −0.07 (slightly cusped) to 0.48. The α's from the least-squares fits are found in Table I and the corresponding T_c's, which are accurate to ±2 mK, are shown in the Fig. 9 phase diagram (○).

The reduced temperatures where the respective ordering peaks begin to round, t_r, are indicated by the lower curve of Fig. 9 (△). These t_r's are compared with the rounding temperatures of ^{4}He ordering peaks at n_c observed on

TABLE I. Set-III coverages and critical exponents.

Run	Coverage (Å^{-2})	α
1	0.0649	−0.067±0.10
2	0.0643	0.016±0.09
3	0.0641	0.055±0.03
4	0.0637	0.24±0.04
5	0.0635	0.37±0.05
6	0.0633	0.48±0.05

ZYX, foam, and Grafoil; see scale for t_r curve. Even far from n_c (data of runs 1 and 2) the t_r's are comparable to those at n_c on Grafoil (Ref. 12) (as was our best peak of set II). The t_r's taken from runs 3, 5, and 6 are about equal to the rounding temperature of the highest ^{4}He peak on foam substrates,[16] while the roundoff temperature taken from run 4 equals that for the published ^{4}He peak on *ZYX*.[14] Evidently, run 4 was taken the closest to n_c among data set III, as anticipated from the heat-capacity-peak—height curve of Fig. 9 (◇) and values of T_c from our phase diagrams. Our $\alpha=0.24\pm0.04$ for the run-4 data and $\alpha=0.37\pm0.05$ for the run-5 data suggest that n_c (where presumably $\alpha=\frac{1}{3}$) lies somewhere between these two coverages.

The critical data and fits for $t<0$ are given in the semilog plot of Fig. 11. Again, data for the various coverages are offset vertically. Data from runs 1, 2, and 3 look about the same as in Fig. 10, but data from runs 4, 5, and 6 lack the strong upward curvature found in the $t>0$ data. These curves were first fitted with the power law given by Eq. (5), but α was found to be about zero and identified as a nonsignificant parameter; i.e., for the run-5 data α was determined to be $0.000\,05\pm0.08$. We therefore set $\alpha=0$ and fitted the critical data for $t<0$ to a logarithmic function and background terms. The T_c's from these fits are shown in the Fig. 9 phase diagram (●), with associated roundoff temperatures indicated (▲) in the lower curve of that figure. The T_c's agree closely with those determined for the high-temperature side of their respective peaks, and the t_r's are scattered in the vicinity of t_r for the only $t>0$ log divergence (run-2 data).

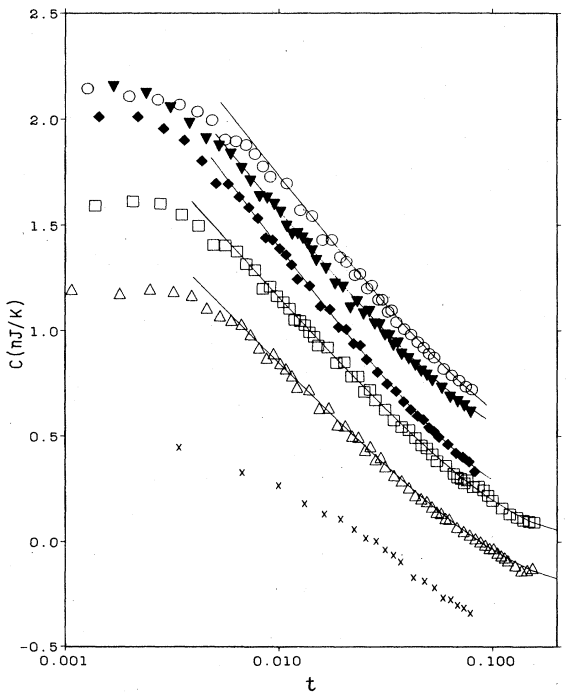

FIG. 11. Set-III low-T fits. Heat capacity (nJ/K) for $t<0$ vs log of reduced temperature. Symbols and shifts are those of Fig. 10. Lines are log fits to data sets.

VII. DISCUSSION

A. Substrate geometry and impurities

Why should ^{4}He ordering transitions on HOPG surfaces be different from those on excellent quality exfoliated graphite surfaces? For one thing, exfoliation is a rough process with inevitable damage to the microcrystals. The HOPG certainly is more uniform than its exfoliated product *ZYX*, possessing ≥ 600 Å crystallites.[6] Gold decoration on cleaved HOPG leaves[26] indicates that $\cong 1\ \mu$m separates surface step planes. The spatial arrangement of our adsorbing surface is also better than for exfoliates. The HOPG calorimeter presents flat crystal facets while *ZYX* possesses high aspect (width to thickness) ratio adsorption chambers with poor vapor-communication channels. Graphite worms and their compressed exfoliates also require vapor communication, additionally relying on physical contact between crystallites for thermal equilibration at low temperatures. These geometry features must cause slight adsorption potential, temperature, and film equilibration variations within the exfoliates which we specifically chose to circumvent by using the HOPG leaf. A major success of this experiment is the observation of a much narrower coverage region, corresponding to a more uniform density for the ordered phase than previously measured (see Fig. 9). An estimate of this geometry effect can be obtained from chemical potentials μ. On the low-coverage side of the phase line, Ecke *et al.*[32] found that a μ/k_B shift of ≈ 1.6 K corresponds to a coverage change of 3.1 %. Since our phase line near n_c is only $\frac{1}{3}$ as wide as the phase line on exfoliates, a chemical-potential spread of 1 K comes from the geometry effects described above. This μ/k_B variation is somewhat larger than the 0.2-K adsorption-potential-energy spread found by Ecke and Dash[13] for the ^{4}He melting curve on foam. There, the high zero-point energy of the helium atoms helps to anneal out variations in adsorption potential.

Surface impurities on HOPG crystallites behave somewhat differently than within exfoliated graphite samples. Baking to 300 °C provides sufficient cleaning of natural crystals that sharp adsorption LEED patterns are obtained.[7] Exfoliates have traditionally been cleaned to 475 °C.[16] It is generally accepted that heating to 800 °C, as was done for our Grafoil ballast, drives off all contaminants from the graphite surface.[12] The heater-resistance value of our calorimeter limited bakeout to about 170 °C, with the entire cell out-gassed at 240 °C. The large phase space above our leaf enhances desorption efficiency, but desorption implies considerable prior surface mobility. This mobility affects the quality (topology) of surface impurities, rather than just the quantity of impurity. The shift to edges and corners, allowing the basal surfaces to "come clean," should be more efficient for exfoliates, with their numerous high-adsorption-potential regions, than for HOPG. Thus, an equal helium adsorption potential of calorimeter and Grafoil ballast (Fig. 5 inset) does not lead to surfaces of exactly equal coverage (Fig. 9).

Peak rounding is an excellent measure of adsorbate crystallite size on good basal-plane regions. The set-III

data from run 4 near n_c shows size limitations comparable to those on ZYX surfaces. Since gold decoration indicates very large HOPG crystallite sizes, we conclude that our peaks, unlike those on the exfoliates, are still impurity- rather than size-limited. This difference should have implications for domain-wall movement and pinning in the region of the ordering transition.

B. Peak shape

The values of α and α', obtained from critical analysis results, clearly demonstrate an asymmetry of the ^{4}He ordering peak for films adsorbed on the HOPG leaf. For $T > T_c$ the ordering peak grows from a slightly cusped anomaly above n_c to near the three-state Potts model value of $\alpha = \frac{1}{3}$ at n_c, growing even stronger to $\alpha = 0.48$ just below n_c. For $T < T_c$ the specific heats at all coverages increase logarithmically, therefore following Ising model behavior. Peak Q is nearly symmetric, however, yielding $A^+/A^- = 0.93$ for the logarithmic amplitude ratio.

A symmetric logarithmic peak with $A^+/A^- \sim 0.46$ has been observed for ^{4}He adsorbed on krypton-plated graphite.[16] The preplating alters the substrate-well mosaic from triangular to honeycomb, causing a change in character of the ordering transition from Potts to Ising-like and raises T_c from 2.92 to 3.11 K. Our peaks taken near n_c have *both* Ising and Potts attributes, yet the separate determinations of T_c and T_c' are each consistent with Potts-model behavior.

The peak's profile changes for coverages away from n_c. This is explained as a Fisher renormalization effect.[33] Experimental data are usually acquired for fixed area and coverage, while critical analyses should be performed at fixed chemical potential. Fisher argued that these differences are unimportant beyond a crossover point in reduced temperature. We have already seen in Fig. 8 that the peak wings far from T_c overlap reasonably well, as expected in the unrenormalized regime. A more important property for $n \neq n_c$ is the renormalization of critical exponents from α to $\alpha_R = \alpha/(\alpha - 1)$ for t's less than the crossover temperature. Far from n_c, the Potts exponent $\alpha = \frac{1}{3}$ will be a cusp having $\alpha_R = -\frac{1}{2}$. We have demonstrated that α changes smoothly from $\alpha = -0.07$ at $n = 1.02 n_c$ to $\alpha \sim \frac{1}{3}$ at $n \approx n_c$, in agreement with Fisher renormalization predictions. Surprisingly, the value $\alpha = 0.48$ for run 6 does not agree with this renormalization. When α is quite small the renormalization regime should be very close to T_c, and one would not expect α_R to observably change from its α value at n_c. Our α's are all equal to zero for $t < 0$, irrespective of coverage.

A careful analysis of Fisher renormalization effects for the ^{4}He peak on foam has recently been completely by Ecke *et al.*[32] They find that slight changes in chemical potential have profound effects on peak height away from n_c. Although corrections must be added to the data of Figs. 10 and 11, the vapor pressure is vanishingly small so chemical potentials are not yet mapped out well enough in coverage and temperatures near n_c to perform quantitative calculations. We believe, however, that data from runs 4 and 5 were taken sufficiently close to n_c that the observed asymmetry can be accepted as a significant film property. We do not presently understand the relation of the symmetry-causing mechanism to impurity effects.

VIII. CONCLUSIONS

We have succeeded in observing and analyzing some properties of the ordering transition for ^{4}He adsorbed on a single cleaved crystal of HOPG. The film adsorption potential and coverage were found to be those of the associated Grafoil ballast. For set II, peak shape and rounding were shown to be similar to those measured for ^{4}He ordering on Grafoil. We searched for, but did not find, a melting signature for films near monolayer completion. Our very narrow ordered-phase region was interpreted as geometry differences between the exfoliated and HOPG adsorption surfaces. The reduced temperature at rounding for the heat-capacity peak of data set III, run 4 corresponds to t_r for ^{4}He ordering on ZYX. The near ideality of HOPG surfaces suggests that our peaks are still impurity-limited. Variations in α as n_c is approached are understood as Fisher renormalization effects. However, the peak asymmetry and the large value for α found during run 6 are not presently understood.

We are designing a natural-crystal calorimeter which will extend microscrystalline sizes beyond current impurity levels and eventually even beyond HOPG limitations. Such a natural-crystal calorimeter would complement single-surface low-temperature diffraction experiments.[7,8]

ACKNOWLEDGMENTS

We are indebted to M. W. H. Chan, who participated fully in developing the ac microcalorimetry techniques and assisted in the initial data collection and analysis (Ref. 10). We appreciate comments by A. N. Berker, J. G. Dash, S. C. Fain, Jr., M. Schick, and M. Wortis. We thank the Rackham Graduate School for partial support.

---

*Present address: Department of Electrical Engineering, Princeton University, Princeton, NJ 08544.

[1] A. Thomy and X. Duval, J. Chim. Phys. **66**, 1966 (1969).

[2] M. Bretz and J. G. Dash, Phys. Rev. Lett. **26**, 963 (1971).

[3] Worms is an uncompressed exfoliate of graphite natural single crystals, while foam and Grafoil are partially compressed and rolled exfoliates, respectively. Grafoil is marketed by Union Carbide, Inc., while a similar product, Papyex, is manufactured by Carbone-Lorraine. ZYX is a carefully exfoliated HOPG single crystal, also manufactured by Union Carbide.

[4] A controlled exfoliate of natural single crystal. For details, see R. Clarke, P. M. Horn, S. E. Nagler, and T. F. Rosenbaum, J. Appl. Phys. **55**, 1231 (1984).

[5] H. Taub, K. Carneiro, J. K. Kjems, L. Passel, and J. P. McTague, Phys. Rev. B **16**, 4551 (1977).

[6] R. J. Birgeneau, P. A. Heiney, and J. P. Pelz, Physica (Utrecht)

109&110B, 1178 (1982).
[7]M. D. Chinn and S. C. Fain, Jr., Phys. Rev. Lett. **39**, 146 (1977).
[8]K. L. D'Amico, D. E. Moncton, E. D. Specht, R. J. Birgeneau, S. E. Nagler, and P. M. Horn, Phys. Rev. Lett. **53**, 2250 (1984).
[9]P. F. Sullivan and G. Seidel, in Proceedings of the 1966 Low Temperature Calorimetry Conference (Otaniemi, Finland) [Ann. Acad. Sci. Fenn., Ser. A **210**, 58 (1966)]; Phys. Rev. **173**, 679 (1968).
[10]J. H. Campbell, M. Bretz, and M. W. H. Chan, in Proceedings of the International Conference on Low Temperature Physics—LT-17, Karlsruhe, Gemany (1984) (unpublished), p. 1165. Also see *Ordering in Two Dimensions,* edited by S. K. Sinha (North-Holland, New York, 1980), p. 295.
[11]S. V. Hering, S. W. VanSciver, and O. E. Vilches, J. Low Temp. Phys. **25**, 793 (1976).
[12]M. Bretz, J. G. Dash, D. C. Hickernell, E. O. McLean, and O. E. Vilches, Phys. Rev. A **8**, 1589 (1973).
[13]R. E. Ecke and J. G. Dash, Phys. Rev. B **28**, 3738 (1983).
[14]M. Bretz, Phys. Rev. Lett. **38**, 501 (1977).
[15]S. Alexander, Phys. Lett. **54A**, 353 (1975).
[16]M. J. Tejwani, G. Ferreira, and O. E. Vilches, Phys. Rev. Lett. **44**, 152 (1980).
[17]M. P. M. den Nijs, J. Phys. A **12**, 1857 (1979).
[18]D. A. Huse and M. E. Fisher, Phys. Rev. Lett. **49**, 793 (1982).
[19]D. Nagle, Ph. D. thesis, Penn State University, 1972 (unpublished).
[20]C. E. Drumheller, in *Transactions of the 7th National Vacuum Society Symposium, 1960* (Pergamon, New York, 1961), p. 306; M. Priest, Vacuum **12**, 301 (1962).
[21]Electrodag 501 is a graphite and carbon powder suspension in an organic polymer binder. Product of Acheson Colloids, Inc., Port Huron, MI 48060.
[22]*The 1958 ^{4}He Scale of Temperature,* edited by F. G. Brickwedde, U. S. National Bureau of Standards Monograph No. 10 (U.S. GPO, Washington, D. C., 1960).
[23]Cromemco *Z* 80 System Two, Cromemco, Inc., 280 Bernardo Ave., Mountain View, CA 94040.
[24]"Dynamic" lock-in amplifier model 393, Ithaca, Inc., 735 W. Clinton St., Ithaca, NY 14850.
[25]R. L. Elgin and D. L. Goodstein, in *Proceedings of the International Conference on Low Temperature Physics—LT-13,* edited by K. D. Timmerhaus, W. J. O'Sullivan, and E. F. Hammel (Plenum, New York, 1974), Vol. 2, p. 175.
[26]For details, see J. H. Campbell, Ph.D. thesis, University of Michigan, 1984 (unpublished).
[27]F. L. Lederman, M. B. Salamon, and L. W. Shacklette, Phys. Rev. B **9**, 298 (1974).
[28]L. P. Kadanoff, W. Götze, D. Hamblen, R. Hecht, E. A. S. Lewis, V. V. Palclauskas, M. Raye, J. Swift, D. Aspnes, and J. Kane, Rev. Mod. Phys. **39**, 395 (1967).
[29]However, M. Bretz, Ph.D. thesis, University of Washington, 1971 (unpublished), gives $\alpha=0.3$.
[30]T_c for the *ZYX* data was increased by 20 mK to compensate for an apparent calibration error in Ref. 14.
[31]BBN Software Products Corp., 1 Alewife Rd., Cambridge, MA 02140.
[32]R. E. Ecke, Q. S. Shu, T. S. Sullivan, and O. E. Vilches, Phys. Rev. B **31**, 448 (1985).
[33]M. E. Fisher, Phys. Rev. **176**, 257 (1968); M. E. Fisher and P. E. Scesney, *ibid.* A **2**, 825 (1970).